PHYSICAL REVIEW D VOLUME 8, NUMBER 5 1 SEPTEMBER 1973

Pion and Proton Inclusive Distributions in the Diffractive-Excitation Model*

J. P. Holden† and D. C. Robertson‡
Institute of Theoretical Science, University of Oregon, Eugene, Oregon 97403
(Received 18 September 1972)

The leading one-particle distributions for the inclusive reaction $pp \to cX$ ($c = p, \pi^+$) calculated in the diffractive-excitation model (DEM) are compared with the new CERN Intersecting Storage Rings data. For the pion distribution we show that a single Gaussian decay distribution, $\exp(-\lambda k^2)$, even with the added assumptions of momentum conservation and off-axis scattering of the clusters, is unable to fit the data. We then show that a pion decay distribution given by a sum of two Gaussians does fit both the fixed-x and fixed-$P_\perp{}^2$ distributions. The proton distributions are well fitted by a single Gaussian decay distribution. The proton spectrum exhibits a broad dip at $x \approx 0.85$ which is naturally explained in the DEM as protons emanating from a cluster ($x \lesssim 0.8$) and unexcited protons recoiling against a massive cluster ($x \gtrsim 0.9$).

I. INTRODUCTION

The diffractive-excitation model (DEM), as formulated by Hwa,[1] Hwa and Lam,[2] and Jacob and Slansky,[3] has successfully explained a broad range of experimental observations on one-particle and two-particle inclusive reactions. It is compatible with the (apparently) logarithmic growth of average pion multiplicity with energy[1] and makes essentially no-parameter fits to the single-pion inclusive x distributions[2]; it also makes very definite (and distinctive) predictions for the two-particle longitudinal-momentum correlations.[4] By using a combination of diffractive excitation and Regge exchange for the throughgoing (unexcited) proton, a flat proton spectrum ($d\sigma/dx$) is obtained.[5,6] Longitudinal- and transverse-momentum correlations in the proton spectrum have also been studied.[7] Finally, the DEM has been used successfully to calculate particle production ratios as functions of longitudinal momentum.[8]

The recent results on pp collisions,[9] which show a sharp deviation in the charged-particle multiplicity distribution at 205 GeV/c from the naive expectations of both the DEM ($\sigma_n \sim 1/n^2$) and the multiperipheral model [$\sigma_n \sim (\bar{n})^n e^{-\bar{n}}/n!$, $\bar{n} \sim \ln s$] are also understandable[10] in the DEM as arising from exponential damping of high-multiplicity events due to finite-energy effects which, when taken appropriately into account, yield excellent agreement with the multiplicity distribution and the energy dependences of $\sigma(n_c)$ and the average charged-particle multiplicities $\langle n_c \rangle$ and $\langle n_c(n_c-1) \rangle$.

We present here an analysis within the framework of the DEM of the available data on $pp \to cX$ ($c = \pi, p$) at 28 GeV/c (Ref. 11) and at CERN Intersecting Storage Rings (ISR) energies.[12,13] We analyze, and remove as far as possible, the simplifying but rather gross approximations previously used in confronting the DEM with the data.[14] We attempt to find a consistent set of parameters for the simultaneous analysis of the longitudinal- and transverse-momentum distributions for both pions and protons.

The single-pion inclusive distribution over the transverse momentum $P_\perp{}^2$ at fixed $x = P_\parallel / \frac{1}{2}\sqrt{s}$ shows a noticeable break around $P_\perp{}^2 \sim 0.2$ (GeV/c)^2; the distributions for larger $P_\perp{}^2$ fall much more slowly than would be expected from a single Gaussian fit to the small-$P_\perp{}^2$ region. Motivated by this observation and the apparent x dependence of the widths of the transverse-momentum(Gaussian) distributions,[11] we have relaxed the constraint requiring the excited clusters in the DEM to remain on the initial beam axis; the off-axis cluster momentum therefore contributes a systematic component to the transverse momentum of the pion and proton distributions, as well as making the effective widths of the distributions x-dependent. As discussed later, we find that off-axis scattering has little effect on the one-particle distributions except at the largest $P_\perp{}^2$ and x values, which are dominated by the lightest clusters; specifically, this alteration is inadequate to explain the two-slope structure of the pion transverse-momentum distribution.

The proton spectrum ($d\sigma/dx$) obtained from experiments at 20–30 GeV/c is fairly flat[15] for large x ($x \gtrsim 0.5$), while at ISR energies there is some indication that the proton spectrum has a broad dip at $x \sim 0.85$.[13] The lower-energy data were previously analyzed in the DEM using the assumption that the proton spectrum for $x \lesssim 0.5$ is determined by Regge exchange between the observed proton and the very massive object representing the remainder of the observed proton's cluster, the other cluster, and the diffractive exchange.[5,6] Here we make the assumption that diffractive ex-

citation dominates at all x (single and double excitation being automatically included). This leads naturally to a broad dip in the proton spectrum produced by the different contributions of protons emanating from an excited cluster ($x \lesssim 0.8$) and unexcited protons recoiling forward against a massive cluster ($x \gtrsim 0.9$).[16]

In Sec. II we briefly outline the derivation of the one-particle inclusive distributions and discuss some of the simplifying assumptions and approximations in the DEM. In Secs. III and IV we present out analyses of the pion and proton distributions.

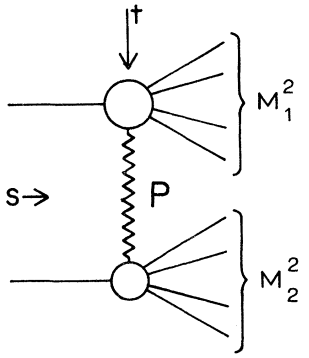

FIG. 1. Double excitation of two clusters in the DEM.

II. FRAMEWORK

The basic assumptions of the DEM can be characterized as follows[1,2]: (1) During a high-energy inelastic collision, very massive excited states (clusters, novas,[3] or fireballs) are formed by diffractive excitation via exchange of the vacuum trajectory, taken here as a weak, fixed singularity at $j = 1$ (Fig. 1); and (2) these massive objects decay via the isotropic emission of pions in their respective cluster rest frames. As discussed in Refs. 2 and 3, the cross section for the diffractive excitation of a proton into a high-mass cluster can be shown to be

$$\frac{d\sigma}{dM} \sim 1/M^2. \tag{1}$$

This result follows from Regge assumptions at large M^2 plus duality, in the absence of triple Pomeranchukon coupling. For the excitation of a massive cluster in an off-axis configuration, characterized by a squared momentum transfer t, we take the form

$$\frac{d^2\sigma}{dt\,dM} = \frac{\gamma(M)}{M^2} e^{2B_0 t}, \tag{2}$$

where the exponential factor represents a diffraction peak and $\lambda(M)$ takes account of threshold effects in the missing-mass spectrum. We parametrize B_0 as [10]

$$B_0 = b_0 + b_1/M^2. \tag{3}$$

Such a form is suggested by data and by analogy with two-body and quasi-two-body reactions. The $1/M^2$ dependence in Eq. (2) is crucial to the model, leading to the (apparently) observed logarithmic growth with energy of the average pion multiplicity. The DEM, being expected to be valid principally at large multiplicity (and so large cluster mass M), can say nothing about the threshold factor $\lambda(M)$ other than requiring $\lambda(M) \to$ constant as $M \to \infty$. In our work we have simply taken $\lambda(M) = A\Theta(M - M_0)$, where A is an adjustable normalization constant and M_0 is a (slightly) adjustable mass constrained to be roughly equal to the expected location of the peak in the missing-mass spectrum, $M_0 \approx 1.5$ GeV/c^2.[3]

The massive clusters are assumed to decay via isotropic emission of pions in their respective cluster rest frames.[17] For simplicity of discussion, we assume here that the pion and proton decay distributions are given by Gaussian distributions in the three-momenta of the particles in the cluster frame, of the form $k_0 e^{-\lambda k^2}$, where $k = |\vec{k}|$ = particle momentum in the cluster frame, and $k_0^2 = m^2 + \vec{k}^2$. Then the decay distribution function for the decay of a cluster of mass M_1 into a proton with (longitudinal, transverse) momentum $\vec{k}_p = (\vec{k}_{p\parallel}, \vec{k}_{p\perp})$ and n pions with momenta $\vec{k}_i = (\vec{k}_{i\parallel}, \vec{k}_{i\perp})$ is given by

$$G_n(k_p; k_1 \cdots k_n) d^3k_p \cdots d^3k_n = \left(\frac{\lambda}{\pi}\right)^{3n/2} \left(\frac{\beta}{\pi}\right)^{3/2} e^{-\beta_0 k_p^2} d^3k_p \left(\prod_{i=1}^{n} e^{-\lambda_0 k_i^2} d^3k_i\right) \delta^{(3)}\left(\vec{k}_p + \sum_i \vec{k}_i\right), \tag{4}$$

where λ_0 (β_0) determines the average energy of a pion (proton) in the cluster and the δ function imposes momentum conservation on the cluster decay. Energy conservation is only statistically satisfied, as discussed more fully below. The constants λ and β are defined below.

After integrating over the unobserved particles, we obtain[6] the one-particle decay distributions

$$G_{n\pi}(\vec{k}) d^3k = \left(\frac{\lambda}{\pi}\right)^{3/2} e^{-\lambda k^2} d^3k, \tag{5}$$

$$G_{np}(\vec{k}) d^3k = \left(\frac{\beta}{\pi}\right)^{3/2} e^{-\beta k^2} d^3k, \tag{6}$$

where, due to momentum-conservation effects,

$$\lambda = \lambda_0\left[1+\frac{\beta_0}{\lambda_0+(n-1)\beta_0}\right], \quad \beta = \beta_0+\lambda_0/n. \tag{7}$$

The average pion (proton) energy in the cluster frame is determined by λ (β) and is well approximated by[18]

$$\begin{aligned} E_\pi &= \langle k_0\rangle \simeq \langle k_0^2\rangle^{1/2} = (1.5/\lambda + m_\pi^2)^{1/2}, \\ E_p &= \langle k_{p0}\rangle \simeq \langle k_{p0}^2\rangle^{1/2} = (1.5/\beta + m_p^2)^{1/2}. \end{aligned} \tag{8}$$

As discussed in Refs. 1 and 6, energy conservation is satisfied only on the average, so that the cluster mass is given by $M = nE_\pi + E_p$. Using this average energy conservation, we approximate the sum over the n-particle cross sections by an integral over dn:

$$\sum_n n\int_{M_0}^\infty dM\ \delta(M-nE_\pi-E_p) \to \int_{M_0}^\infty dM\, n(M)/E_\pi. \tag{9}$$

This procedure makes n a continuous variable. Since Eq. (8) clearly shows that E_π and E_p are functions of n (through λ and β), the right-hand side of Eq. (9) should actually be written

$$\int_{M_0}^\infty dM \frac{\bar n(M)}{\left|\left(d/dn[nE_\pi(n)+E_p(n)]\right|_{n=\bar n(M)}\right.},$$

where $M-\bar nE_\pi(\bar n)-E_p(\bar n)=0$. Although this refinement has been included in our numerical programs (it is a small effect), we will forgo writing the full form here and just write Eq. (9) as shown.

All our calculations are done in the $s\to\infty$ limit, yielding the following *limiting* invariant one-particle distributions:

$$\begin{aligned} f_\pi(x,P_\perp) &\equiv x\frac{d^2\sigma}{dx\,dP_\perp^2} \\ &= A\int_{M_0}^\infty dM\,\frac{d^2\sigma}{dM\,dt}G_{n\pi}(M,\vec p)k_0 n(M)\,dt\,d\varphi, \end{aligned} \tag{10}$$

$$f_p(x,P_\perp) = A'\int_{M_0}^\infty dM\,\frac{d^2\sigma}{dM\,dt}\,G_{np}(M,\vec p)k_0\,dt\,d\varphi. \tag{11}$$

Here k_0 = particle energy in the cluster frame, and M_0 = the mass of the lightest cluster. The M dependence of G_π and G_p enters via the n dependence and the statistical treatment of energy conservation. Expressed in c.m. variables $(x, P_\perp)$ we have

$$\begin{aligned} 2k_0 = xM + \frac{\mu_\perp^2}{xM} - \frac{2P_\perp}{M}\sqrt{-t}\,\cos\varphi + \frac{x}{M}(-t) \\ + O((-t)^{3/2}) \end{aligned} \tag{12}$$

where φ is the azimuthal angle of $\vec P_\perp$ in the c.m. system and t is the square of the momentum transfer to the cluster as a whole.[19] The zenith angle is measured from the beam direction. This is expected to be small because of the diffraction peak contained in $G_\pi(M,\vec p)$ and $G_p(M,\vec p)$. The integrations over $d\varphi$ and dt can be done in closed form[20] if only the terms written explicitly in Eq. (12) are kept. One finds

$$\begin{aligned} f_\pi(x,P_\perp^2) = A\int_{M_0}^\infty dM\,\frac{n(M)}{M^2}\tfrac{1}{2}\left(xM+\frac{\mu_\perp^2}{xM}\right)h(\lambda,x,P_\perp^2,M) \\ \times\exp\{-\tfrac{1}{4}\lambda[xM-\mu_\perp^2/(xM)]^2 \\ -\lambda P_\perp^2 + D\}, \end{aligned} \tag{13}$$

where

$$D = \tfrac{1}{4}\lambda^2 P_\perp^2\alpha^2/c, \tag{14}$$

$$h(\lambda,x,P_\perp^2,M) = \frac{1}{c}(1-\delta)^{-1/2} \times[1-\delta+x/(M^2\alpha c)+O(1/c^2)], \tag{15}$$

$$\mu_\perp^2 = P_\perp^2 + m_\pi^2, \tag{16}$$

$$\alpha = x+\mu_\perp^2/(xM^2), \tag{17}$$

$$c = 2B_0 + \tfrac{1}{2}\lambda x\alpha + \lambda P_\perp^2/M^2, \tag{18}$$

$$\delta = \lambda P_\perp^2/(M^2 c). \tag{19}$$

$h(\cdots)$ can actually be expressed in closed form, but this polynomial dependence is not significant. Also, M_0 is defined following Eq. (3). The proton distribution is easily obtained from Eq. (13) by setting $n(M)=1$ and letting $\lambda\to\beta$.

III. PION DISTRIBUTIONS

The distribution function given by Eq. (13) has been used to fit the $pp\to\pi^+X$ ISR data of Ratner *et al.*[12] Our fits to the fixed-x and fixed-$p_\perp^2$ distributions are shown in Fig. 2. The values of the parameters used are $\lambda_0 = 6.0\ (\mathrm{GeV}/c)^{-2}$, $\beta_0 = 2.5\ (\mathrm{GeV}/c)^{-2}$, $B_0 = 0.5 + 5/M^2$, and $M_0 = 1.5\ \mathrm{GeV}/c^2$. The fit was normalized to the data at $(x, p_\perp^2) = (0.1, 0.1)$. As might be expected, the pion distributions are insensitive to the proton parameter β_0. The correlations between x and $p_\perp^2$ are due mainly to the Lorentz transformation from the cluster rest frame to the over-all c.m. system given by Eq. (12). The effects of the off-axis scattering are contained largely in the D term, Eqs. (13) and (14). These correlations are small, as evidenced by comparison of the fit for $b_0=\infty$ (on-axis scattering)[19,21] and for $b_0 = 0.5$. Evidently, the DEM with a single Gaussian decay distribution cannot accurately reproduce the transverse-momentum dependence of the data, and the off-axis scattering of the clusters is insufficient to improve the fits significantly.

The failure of the single Gaussian form to fit the data can be understood by returning to the

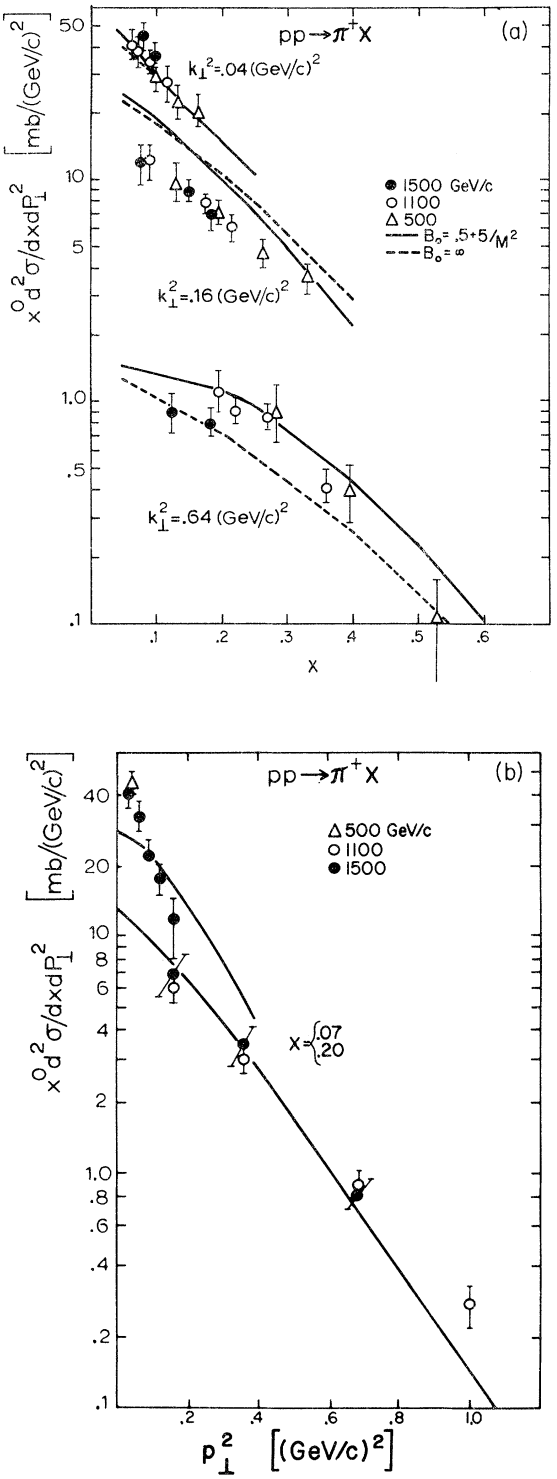

FIG. 2. (a) Pion distribution for fixed x. Data are from Ref. 12. The DEM predictions for a single Gaussian decay distribution with off-axis scattering ($B_0 = 0.5 + 5/M^2$) and momentum conservation are shown by the solid curves. The on-axis case is shown by the dashed curves. (b) Pion distribution for fixed $P_\perp{}^2$.

simplest case of on-axis scattering with no momentum conservation. In this case, the integral over cluster mass in Eq. (13) can be done exactly[22] to yield

$$f_\pi(x,P_\perp{}^2) = Ae^{-\lambda_0 P_\perp{}^2}\,\mathrm{erfc}\left[\tfrac{1}{2}\sqrt{\lambda_0}\,(xM_0 - \mu_\perp{}^2/xM_0)\right], \tag{20}$$

where erfc $(x) \equiv 1 - \mathrm{erf}\,(x)$ is the complementary error function and $\mu_\perp{}^2 = P_\perp{}^2 + m_\pi{}^2$ is the transverse pion mass. The x distributions for fixed $P_\perp{}^2$ are shown in Fig. 3. The parameter λ_0 governs both the slope of the distribution in x and the relative magnitudes of the distributions for different $P_\perp{}^2$. For $\lambda_0 = 7.5\ (\mathrm{GeV}/c)^{-2}$ this simple form gives the shapes of the distributions in x for fixed $P_\perp{}^2$, but fails to give their relative magnitudes correctly. Looking to the data, one sees that the relative magnitudes of the distributions for fixed $P_\perp{}^2$ follow basically from $\exp(-7P_\perp{}^2)$; this is just the above value of λ_0. There is, however, additional $P_\perp{}^2$ dependence in the distribution arising from the transverse mass term $\mu_\perp{}^2$ in the argument of the error function. From the asymptotic form of the error function, this piece contributes a dependence (for x not too small) of the form $\exp(\frac{1}{2}\lambda_0 P_\perp{}^2)$. It is this factor which is responsible for the "bunching" of the $P_\perp{}^2 = 0.04$ and $P_\perp{}^2 = 0.16$ distributions;

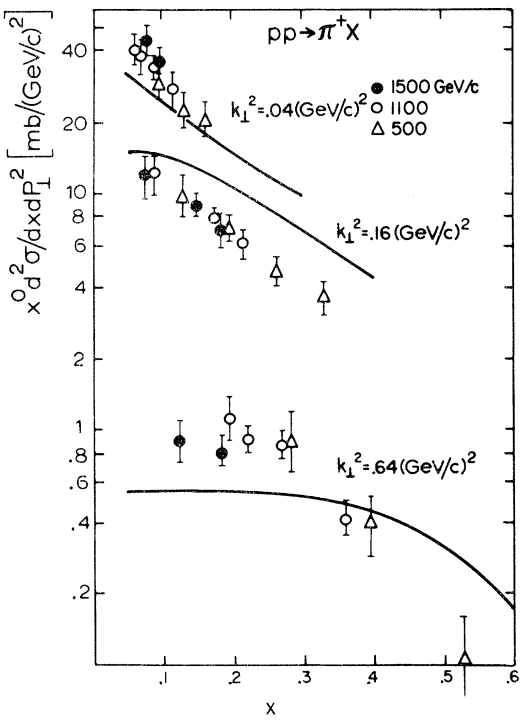

FIG. 3. Fixed-$P_\perp{}^2$ distribution given by the erfc function defined in Eq. (20) with no momentum conservation.

the effect persists through any additional refinements such as momentum conservation and off-axis scattering contributions.

Momentum conservation only affects the lighter clusters, as seen in Eq. (7) by the dependence of λ on the cluster mass M, which is roughly proportional to n. These effects can be seen by comparing Fig. 2 (for $B_0=\infty$, which includes momentum conservation) with the simple distribution in Fig. 3.

Gordon and Lam[6] have also analyzed the effects of momentum conservation on the single-particle distributions. Their results are similar to those of Fig. 2, with the exception of the "bunching" of the distributions at $P_\perp{}^2=0.04$ and $P_\perp{}^2=0.16$. The origin of this difference can be traced to the different approximations used by Gordon and Lam in the statistical treatment of the energy-conservation δ function. Since energy conservation is imposed "only on the average," we make the replacement

$$\delta\left(k_{p0}+\sum_{i=1}^{n}k_{i0}-M\right)\to\delta(E_p+nE_\pi-M). \tag{21}$$

The energies used here [E_p and E_π are defined by Eq. (8)] are *average* energies, and n must be taken as continuous. As mentioned in footnote 10 of Ref. 6, the "average energy" used by Gordon and Lam is given by

$$E_\pi\simeq\langle k_0{}^2\rangle^{1/2} = (1/2\lambda+P_\perp{}^2+m_\pi{}^2)^{1/2}. \tag{22}$$

It is this factor of $P_\perp{}^2$ in E_π which gives added weight to those pions with small transverse momenta and eliminates the "bunching." Note, however, that this means that, if one observes a pion with $P_\perp{}^2=0.04$ (GeV/c)^2 which comes from a massive cluster of 20 pions (say), then all 20 pions would have an average transverse momentum of $P_\perp{}^2=0.04$. We feel that such an assumption is artificial and violates the statistical spirit of the treatment of decay distributions in DEM. Therefore, we are led to conclude that a single Gaussian decay distribution is inadequate for all $P_\perp{}^2$ and not just for large $P_\perp{}^2$ as asserted in Ref. 6. This is also apparent from comparing the model's $P_\perp{}^2$ distributions with the data taken at fixed x (see Fig 2).

Faced with this failure, we have tried a number of other *single-component* distributions without notable success. For example, a simple exponential form

$$\phi_\pi\sim k_0 e^{-\lambda|\vec{k}|} \tag{23}$$

leads to an average pion energy in the cluster rest frame of

$$E_\pi\simeq\langle k_0{}^2\rangle^{1/2} = [m_\pi{}^2+3(4/\lambda^2)]^{1/2}, \tag{24}$$

and an average transverse momentum

$$\langle k_\perp{}^2\rangle = 2(4/\lambda^2). \tag{25}$$

In attempting to fit the data, the x distributions at fixed $P_\perp{}^2$ require $\lambda\simeq 3.5$ (GeV/c)$^{-2}$, while the small value of observed transverse momenta ($\langle k_\perp\rangle\sim 350$ MeV/c) requires $\lambda\simeq 7.0$ (GeV/c)$^{-2}$. Again, momentum conservation and off-axis scattering effects are insufficient to improve the situation (momentum conservation actually makes the fits worse by an order of magnitude). We conclude that a single-component decay distribution is definitely ruled out by the data; at least, any simple and attractive form is excluded by detailed fits to the data.

The ISR data of Ratner *et al.*[12] at fixed x strongly suggest that the pion-decay distribution has a two-component form. A similar fit to data has been carried out by Panvini *et al.*,[11] on the basis of their data on $pp\to\pi^- X$ at 29 GeV/c. If we assume this two-component form for the decay distribution in the cluster frame, the distributions take the form (for n pions and one proton)

$$G_n(k_p\cdots k_n)\sim e^{-\beta_0 k_p{}^2}d^3k_p\left[\prod_{i=1}^{n}d^3k_i\,(e^{-\lambda_1 k_i{}^2}+ce^{-\lambda_2 k_i{}^2})\right] \times\delta^{(3)}\left(\vec{k}_p+\sum_i\vec{k}_i\right) \tag{26}$$

The ISR data suggest $\lambda_1\sim 20$ (GeV/c)$^{-2}$ and $\lambda_2\sim 4$ (GeV/c)$^{-2}$. The relative strength of the two components is determined by the parameter c. Momentum conservation is rigorously enforced by the δ function, but once again energy conservation is imposed only statistically.

Fairly simple approximate expressions for the one-particle distributions arising from Eq. (26) can be obtained by expanding in powers of the parameter

$$\epsilon=(\lambda_2/\lambda_1)^{3/2}/c. \tag{27}$$

We find

$$G_{n\,\pi}(k)\,d^3k = A\,d^3k(e^{-\lambda_1 k^2}+ce^{-\lambda_2 k^2})\exp\left(-\frac{\lambda_2\beta k^2}{\lambda_2+(n-1)\beta}\right)\left[\left(\lambda_1+\frac{\lambda_2\beta}{\lambda_2+n\beta-\beta}\right)^{3/2}+\left(\lambda_2+\frac{\lambda_2\beta}{\lambda_2+n\beta-\beta}\right)^{3/2}\right]^{-1}+O(\epsilon^2). \tag{28}$$

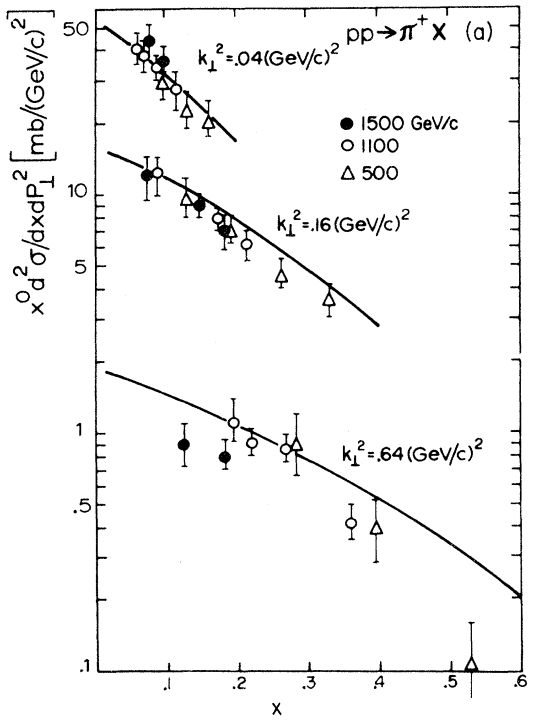

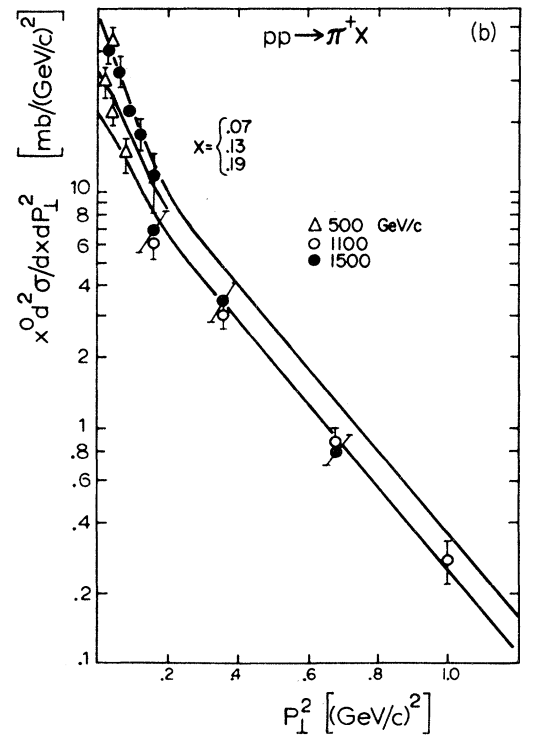

FIG. 4. (a) The one-particle pion distribution for fixed $P_\perp$ given by a two-Gaussian decay distribution as defined in Eq. (28). Data are from Ref. 12. (b) Pion distribution for fixed x.

We used the values $\lambda_1 = 20$ $(\mathrm{GeV}/c)^{-2}$ and $\lambda_2 = 4$ $(\mathrm{GeV}/c)^{-2}$ suggested by the data and varied the parameter c. The results of this analysis are shown in Fig. 4. As anticipated, the fits to the $P_\perp{}^2$ data at fixed x and to the x distributions at fixed $P_\perp{}^2$ are quite good. The parameter $c = 0.15$, and the over-all normalization was chosen to fit the fixed-x data at $(x, P_\perp{}^2) = (0.07, 0.1)$. We have not attempted to find "best" fits, but only searched for a fit compatible with the data using only the statistical assumptions inherent in the DEM. The parameter B_0, which governs the off-axis scattering contributions, was fixed at $B_0 = 6$ $(\mathrm{GeV}/c)^{-2}$. The alternative form $(B_0 = 0.5 + 5/M^2)$ used previously has little effect on the fits and does not alter their qualitative features. Since our results are insensitive to the minimal cluster mass M_0, we have put $M_0 = 1.5$ GeV/c^2.

In Fig. 5 we present the average $P_\perp{}^2$ as a function of x as predicted by the DEM's fit to the ISR data. As discussed in Refs. 6 and 8, the $pp \to \pi^- X$ data[23] are similar to the $pp \to \pi^+ X$ data and can be easily explained by using isospin counting arguments; therefore we do not present a fit here. Likewise, the $pp \to \pi^- X$ data of Ref. 11 are similar to the ISR data, and a fit is not presented here.

IV. PROTON DISTRIBUTIONS

The invariant distribution function for protons is given by Eq. (11).[24] At small x ($x \lesssim 0.5$), the proton distribution is insensitive to all parameters except β_0, which determines the average proton

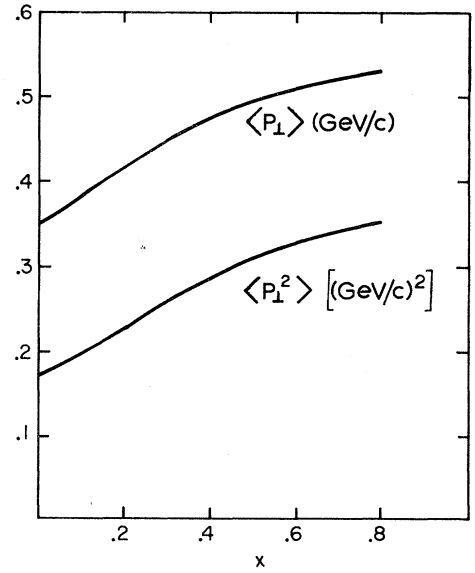

FIG. 5. Seagull effect. Prediction of the DEM for the average value of $P_\perp$ and $P_\perp{}^2$ as a function of x for the pion distribution.

energy in the cluster rest frame. The ISR $P_\perp{}^2$ data at fixed x (Ref. 12) were used to fix β_0 at roughly $\beta_0 = 2.5$ (GeV/c)$^{-2}$. Our fits to the $P_\perp{}^2$ and x distributions, shown in Fig. 6, are good. They are essentially one-parameter fits with one arbitary over-all normalization fixed at $(x, P_\perp{}^2) = (0.2, 0.16)$.

For small x the fixed $P_\perp{}^2$ distribution falls below the data, indicating rather too few protons in this region. The deviation can be understood in terms of protons arising from $\bar{p}p$ production in events with high cluster mass, which we have not included in our analysis. Bertin *et al.*[25] have found that the $(\bar{p}/\pi^-)$ ratio is roughly 8%. If we infer from this an additional contribution of protons in the small-x region — dominated by the high-mass clusters — by assuming a (p/π^+) ratio of 8% also and add this contribution to the proton distribution following from Eq. (11), the agreement with the data for $x \lesssim 0.2$ is quite good. This is indicated by the dashed curve in Fig. 6.

The fit we obtained at small x can be extended to the large-x region and is shown in Fig. 6 (fixed $P_\perp$) and Fig. 7 (fixed angle). The proton spectrum exhibits a peak around $x = 0.5$, falling to zero as x approaches the kinematical boundary $x = 1$.

For $x > 0.5$ the proton spectrum is sensitive to the parameters used to describe the excitation and decay of the lightest clusters (those with only a few pions). The excitation spectrum used here, $d\sigma/dM \sim 1/M^2$, and the cluster decay distribution $G_\pi \sim e^{-\lambda k^2}$ are both expected to be valid for large cluster mass and large multiplicity; thus the detailed nature of the proton distribution for large x is not expected to be adequately reproduced given the rather crude excitation spectrum. In particular, the distribution at large x should be rather sensitive to the threshold factor $\lambda(M)$ in Eq. (2). However, we do expect the qualitative features shown in Fig. 6 to be a firm component of the predictions of the DEM.

Near $x = 1$ the proton distribution exhibits a strong peak arising from throughgoing (unexcited) protons which recoil against a massive cluster. For this process the invariant distribution function

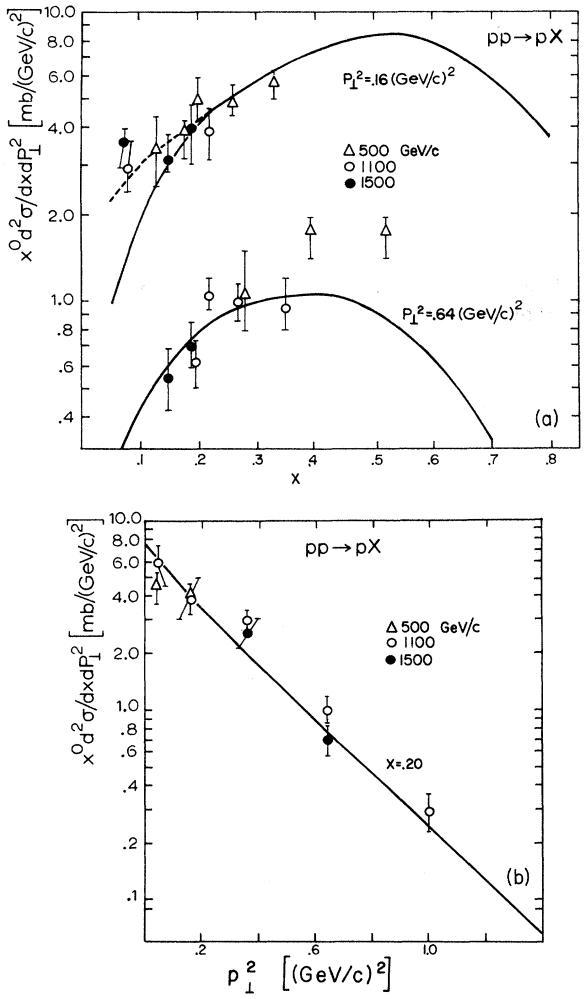

FIG. 6. (a) The one-particle proton distribution for fixed $P_\perp{}^2$. Data are from Ref. 12. The fit, obtained at small x, has been extended out to $x = 0.8$. (b) Proton distribution for fixed x.

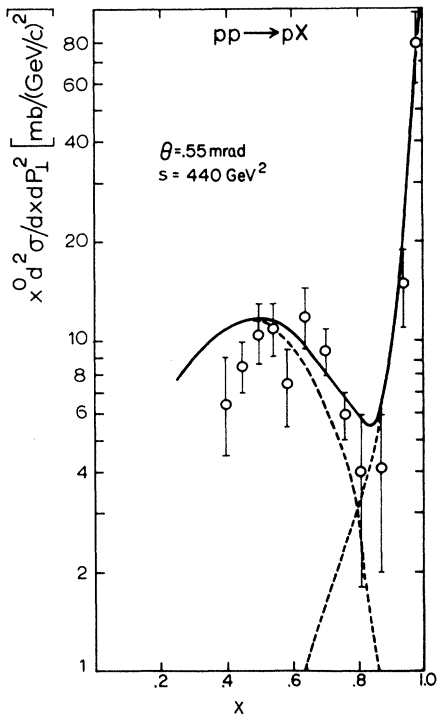

FIG. 7. Comparison of the proton distribution for large x with the fixed-angle data of Ref. 13. The over-all normalizations are arbitrary; the dashed lines are extensions of the cluster and single-proton distributions.

is given by[2,5]

$$f_s(X,P_\perp^2) \sim Be^{2B_0 t}(s/M^3) \simeq (B/\sqrt{s})\exp(-2B_0P_\perp^2/x)(1-x)^{-3/2}, \quad (29)$$

where M is the mass of the excited cluster at negative x and B is an arbitary normalization.

In Fig. 7 we present a comparison of the DEM with the fixed-angle data of Albrow *et al.*[13] The DEM, with its broad peak around $x \sim 0.5$ and a dip for $x \sim 0.85$, is in qualitive agreement with the data.[13] The normalization parameters (B for single excitation and A' for double excitation) were chosen to fit the data for $x \gtrsim 0.9$ and $x \lesssim 0.5$, respectively.

The proton spectrum for both fixed x and fixed $P_\perp^2$ is well described by the DEM with essentially one adjustable parameter, β, the width of the proton decay distribution in the cluster rest frame. The dip at large x is a natural feature of the DEM.

ACKNOWLEDGMENTS

The authors are indebted to Professor R. Hwa for many valuable discussions. One of us (DCR) would like to thank the theory group at SLAC for their hospitality during his summer visit in 1972.

---

*Work supported by the U. S. Atomic Energy Commission under Contract No. AT(45-1)-2230.

†Present address: Department of Physics, McGill University, Montreal 110, Quebec, Canada.

‡Present address: Max-Planck-Institut für Physik und Astrophysik, 8 München 40, Föhringer, Ring 6, West Germany.

[1]R. C. Hwa, Phys. Rev. Lett. 26, 1143 (1971).

[2]R. C. Hwa and C. S. Lam, Phys. Rev. Lett. 27, 1098 (1971).

[3]M. Jacob and R. Slansky, Phys. Rev. D 5, 1847 (1972).

[4]R. C. Hwa, Phys. Rev. Lett. 28, 1487 (1972).

[5]R. C. Hwa, Phys. Lett. 37B, 405 (1971); Phys. Lett. 39B, 251 (1972).

[6]E. M. Gordon and C. S. Lam, Nuovo Cimento Lett. 4, 749 (1972).

[7]R. C. Hwa, Phys. Lett. 39B, 251 (1972).

[8]R. C. Hwa and D. C. Robertson, Phys. Lett. 41B, 502 (1972).

[9]G. Charlton *et al.*, Phys. Rev. Lett. 29, 515 (1972).

[10]R. C. Hwa, Phys. Lett. 42B, 79 (1972).

[11]R. Panvini, in *High Energy Collisions*, edited by C. N. Yang *et al.* (Gordon and Breach, New York, 1970).

[12]L. Ratner *et al.*, Phys. Rev. Lett. 27, 68 (1971); in *Particles and Fields—1971,* proceedings of the 1971 Rochester Meeting of the Division of Particles and Fields of the American Physical Society, edited by A. C. Melissinos and P. F. Slattery (A.I.P., New York, 1971).

[13]M. G. Albrow *et al.* (CERN-Holland-Lancaster-Manchester Collaboration), reported by J. C. H. Sens at the Fourth International Conference on High Energy Collisions, Oxford, 1972 (unpublished); CERN report (unpublished).

[14]Similar calculations are reported in Ref. 5.

[15]J. V. Allaby *et al.*, CERN Report No. 70-12, 1970 (unpublished).

[16]Similar conclusions have been reached by K. Gottfried and O. Kofoed-Hansen [Phys. Lett. 41B, 195 (1972), received when this paper was in preparation].

[17]Such isotropic decays are probably not justifiable in a strict sense for low cluster masses where only a few pions are present and our statistical assumptions are weakest. But Adair has found roughly isotropic decay distributions even here using Monte Carlo methods to impose energy-momentum conservation on cascade decay processes [R. K. Adair, Phys. Rev. D 5, 1105 (1972)].

[18]If we calculate exactly, we find (for the proton, for example)

$$E_p = \langle k_{p0}\rangle = \int G_{np}(k)k_0 d^3k \Big/ \int G_{np}(k)d^3k = m_p^2(\beta/\pi)^{3/2}e^{m_p^2\beta/2}K_1(\tfrac{1}{2}m_p^2\beta),$$

where $K_1(x)$ is a modified Bessel function. Of course, $\langle k_{p0}^2\rangle^{1/2} > \langle k_{p0}\rangle$, but the difference does not exceed 3% for $\beta \geq 1$. For pions, the result is somewhat worse ($\leq 8\%$ for $\lambda \geq 4$), but we use $\langle k_0^2\rangle^{1/2}$ for ease of computation.

[19]Here, and elsewhere, we set $t_0 = t(\theta = 0) = 0$. Since for double excitation $t_0 \sim -M_1^2M_2^2/s$ and we take $s \to \infty$, this approximation is valid for all but the heaviest clusters. That it is not always a good approximation is shown by the calculations of Ref. 10.

[20]We wish to thank Professor R. Mazo for invaluable aid in performing this nontrivial double integral.

[21]Since we take $t_0 = 0$ and normalize each fit to the data, we can rewrite Eq. (2) as

$$\frac{d^2\sigma}{dtdM} = [\bar{A}\theta(M-M_0)/M^2]B_0\exp(2B_0t),$$

and, in the limit as B_0 goes to infinity,

$$\frac{d^2\sigma}{dtdM} = A'\theta(M-M_0)/M^2\delta(t).$$

Hence $B_0 \to \infty$ gives the on-axis scattering result.

[22]See Eq. (32) in R. C. Hwa and D. C. Robertson, Phys. Rev. D 7, 1469 (1973). The form given here assumes $M \cong nE_\pi$.

[23]A. Bertin *et al.*, Phys. Lett. 38B, 260 (1972).

[24]Since we assume there is only one proton in each cluster, the actual E_0 is used and not the statistical E_p of Eq. (8). This is a small correction.

[25]A. Bertin *et al.*, Phys. Lett. 40B, 136 (1972).